Optical and Acoustical Methods in Science and Technology

WO_3–Pd Structure in SAW Sensor for Hydrogen Detection

T. Hejczyk[a] and M. Urbańczyk[b,*]

[a]ENTE Sp. z o.o., Gaudiego 7, 44-100 Gliwice, Poland

[b]Faculty of Electrical Engineering, Silesian University of Technology, B. Krzywoustego 2, 44-100 Gliwice, Poland

In the paper a new sensor structure for surface acoustic wave gas system is presented. A bilayer structure WO_3–Pd thin films may be useful for hydrogen detection in low concentration in air. A bilayer sensor structure of tungsten oxide WO_3 with a very thin catalytic film of palladium on the top has been studied for gas-sensing application at room temperature (about 25 °C) in surface acoustic wave system. The bilayer structure of WO_3 layers with a thickness of about 50 nm, 100 nm and 150 nm was made onto a $LiNbO_3$ *Y*-cut *Z*-propagating substrate by means of the vacuum sublimation method using a special aluminum mask. The vapor source consisted of commercially available WO_3 powder (Fluka 99.9%) and molybdenum heater. The thin palladium (Pd) layer (about 10 nm) was made separately on each WO_3 layer by means of vapor deposition in high vacuum. There have been investigated three structures: 50 nm WO_3 + 10 nm Pd, 100 nm WO_3 + 10 nm Pd and 150 nm WO_3 + 10 nm Pd in three canal surface acoustic wave system with reference oscillator. Numerical results obtained by analysis of the surface acoustic wave gas sensor model have been compared with experimental results.

PACS: 43.25.Fe, 77.65.Dq, 68.35.Iv, 07.07.Df

1. Introduction

Surface acoustic wave (SAW) gas sensors are very attractive due to their great sensitivity in a specific bilayer configuration, as well as low power consumption and frequency measurements. The semiconductor layer on a piezoelectric substrate creates new possibilities for detecting gas in a SAW sensor system by using an acoustoelectric coupling between the surface wave and the structure of the sensor in a high sensitivity region. High sensitivity of the SAW sensors results from the simple fact that most of the acoustic wave energy is concentrated near the crystal surface within one or several wavelengths. Consequently, the surface wave is in its first approximation highly sensitive to any changes of the physical or chemical properties of the thin active sensor layer placed on a wave guide surface [1–15]. As long as the thickness of the sensor layer is less than the wavelength of the surface wave, we can take into consideration the Rayleigh wave type. Otherwise, we have to take into account other types of waves, such as the Love waves which can propagate in layered structures [4]. In our case the whole thickness of the sensor layer structure is smaller than 200 nm. This is less than the wavelength of the Rayleigh wave in our sensor structure ($\lambda = 80$ μm).

From the practical point of view two effects are potentially significant — a change in the mass of the sensor layer and a change of its electrical conductivity. These two effects occur simultaneously. The electric effect in semiconducting sensor layers is usually several times greater than the mass effect. In such a layered sensor structure we can take into account only acoustoelectric interactions in the SAW sensor system as the main detection mechanism. Mass effect is dominant in nonconductive polymer films and simple metal or dielectric films in SAW gas systems [5, 6]. In order to take full advantage of the high sensitivity offered by the SAW sensor through the acoustoelectric effect, the conductivity of the sensor structure must be in some particular range [7, 8].

Any changes in the physical or chemical properties of the thin sensor active layer placed on a surface of the piezoelectric substrate can influence on the SAW propagation, especially on velocity.

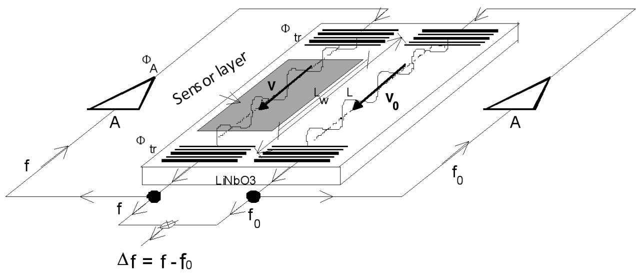

Fig. 1. The basic diagram of the SAW gas sensor as dual delay line oscillator [1].

The basic principle of the SAW sensor with dual line oscillators (sensor and reference one), which is now well known, has been shown in Fig. 1.

2. Theory of the acoustoelectric effect in the piezoelectric-semiconductor layer

The electric effect results from the interaction of the electric potential associated with the surface wave with mobile charge carriers in the sensor layer. The interac-

* corresponding author; e-mail: murbanczyk@polsl.pl

tion of chemically active sensor layer with gas produces changes in their electrical conductivity and mass.

In the case of small disturbances, both mass and electric effect may be considered separately. The total effect of a relative change of the wave vector $\Delta k/k_0$ and the velocity of propagation $\Delta v/v_0$ is the sum of both these component disturbances [9]:

$$\frac{\Delta k}{k_0} \approx \left(\frac{\Delta k}{k_0}\right)_m + \left(\frac{\Delta k}{k_0}\right)_\sigma , \quad (1)$$

where the index σ refers to the change of the wave number by the electric effect, and the index m refers to the change of the wave number by the mass effect. The mass load will be negligible.

The perturbed boundary conditions will be specified in terms of the normalized surface impedance, $z'_E(0)$, or admittance, $y'_E(0)$ [10, 11]. We assume that the surface conductivity σ_0 is not dependent on the frequency of the acoustic wave and the surface admittance, $y'_E(0)$, is only a function of the surface conductivity, σ_0, and velocity of propagation of the SAW, v_0.

$$y'_E(0) = -\mathrm{i} + \frac{\sigma_0}{\varepsilon_0 v_0} , \quad (2)$$

where $\sigma_0 = \sigma d$, σ — bulk conductivity, d — thickness of the semiconductor layer, ε_0 — air electric permittivity.

The interaction effect between the electric potential associated with the acoustic wave and the carriers of the electric charge in this layer leads to a decrease of the velocity. This effect depends on the electromechanical coupling factor K^2. The Ingebrigtsen formula for electrical surface perturbations of the Rayleigh waves takes the following form [10, 12]:

$$\left(\frac{\Delta k}{k_0}\right) = \frac{K^2}{2}\frac{1+\mathrm{i}\,z'_E(0)}{1-\mathrm{i}\,\frac{\varepsilon_p^{\mathrm{T}}}{\varepsilon_0} z'_E(0)} , \quad (3)$$

where

$$K^2 = 2\left(\frac{\Delta v}{v_0}\right)_{\mathrm{sc}} , \quad (4)$$

v_0 is the velocity of the acoustic surface wave, k_0 is the wave propagation factor and the index sc refers to fractional change of velocity produced by shorting the surface potential.

From the Ingebrigtsen formula for single layer we obtain

$$\frac{\Delta v}{v_0} = -\mathrm{Re}\left(\frac{\Delta k}{k_0}\right) = -\frac{K^2}{2}\frac{(\sigma_0)^2}{(\sigma_0)^2 + (v_0 C_S)^2} , \quad (5)$$

where $C_S = \varepsilon_0 + \varepsilon_p^{\mathrm{T}}$ is the sum of the electric permittivity of the wave guide substrate and the environment.

Gas molecules are diffused into a porous thin semiconducting film. We can assume that the molecules made no collision with each other during their passage through the hole, and hence that the molecules moved entirely independently of each other. This kind of diffusion is a Knudsen diffusion [1, 13] which depends on the pore radius, r, and is occurring in pores ranging from 2 nm to 100 nm. The Knudsen diffusion constant, D_{K}, depends on the molecular weight of the diffusing gas, M, the pore radius, r, the temperature, T, and the universal gas constant, R, as follows:

$$D_{\mathrm{K}} = \frac{4r}{3}\sqrt{\frac{2RT}{\pi M}} . \quad (6)$$

Taking into account the Knudsen diffusion and first-order surface reaction we can formulate the well-known diffusion equation [13]:

$$\frac{\partial C_A}{\partial t} = D_{\mathrm{K}}\frac{\partial^2 C_A}{\partial y^2} - kC_A , \quad (7)$$

where C_A is the concentration of target gas, t — time, y — distance from the upper side of the sensor layer, k is the rate constant of the chemical reaction.

Solving this equation in steady state conditions we obtain profile of the gas molecules concentration in sensor layer [1, 13]:

$$C_A = C_{A,S}\frac{\cosh(y\sqrt{k/D_{\mathrm{K}}})}{\cosh(D\sqrt{k/D_{\mathrm{K}}})} , \quad (8)$$

where $C_{A,S}$ is the target gas concentration outside the semiconductor film at the surface.

The gas concentration inside the semiconductor film is not constant. Now we make an assumption that the electrical conductance $\sigma(y)$ of the thin sheet exposed to the target gas is linear to the gas concentration (C_A) inside it [13]:

$$\sigma(y) = \sigma_0(1 \pm aC_A), \quad (9)$$

where σ_0 is the layer conductance in air, a is the sensitivity coefficient.

The profile of gas concentration in a semiconducting sensor layer changes with the distance from the piezoelectric substrate. To analyze such a sensor layer in SAW gas sensor we assumed that the film is a uniform stack of infinitesimally thin sheets with a variable concentration of gas molecules and consistently with a different electric conductance. In our paper [1] we have shown results of the exact analysis of acoustoelectric interaction in such case [13]. From the Ingebrigtsen formula for n sublayers we obtained the following expression for the change of velocity vs. conductivity [1]:

$$\frac{\Delta v}{v_0} = -\mathrm{Re}\left(\frac{\Delta k}{k_0}\right) = -\frac{K^2}{2}\frac{\sigma_{\mathrm{CS}}^2\left[1+\sum_{i=1}^{n-1} f(y_i,\sigma_{\mathrm{CS}})\right]^2}{\sigma_{\mathrm{CS}}^2\left[1+\sum_{i=1}^{n-1} f(y_i,\sigma_{\mathrm{CS}})\right]^2 + \left[1+\sum_{i=1}^{n-1} g(y_i,\sigma_{\mathrm{CS}})\right]^2 (v_0 C_S)^2} , \quad (10)$$

where $\sigma_{\mathrm{CS}} = \sigma_0$ is the surface conductivity of the sublayer with the thickness d, $i = 1, 2, 3, \ldots\ n$, n — quantity of sublayers and

$$f(y_i,\sigma_{CS}) = \sum_{i=1}^{n-1} \frac{1-[\tanh(ky)]^2}{[1+\tanh(ky)]^2 + \left[\tanh(ky)\frac{\sigma_{CS}}{\varepsilon_0 v_0}\right]^2}, \tag{11}$$

$$g(y_i,\sigma_{CS}) = \sum_{i=1}^{n-1} \frac{1+[\tanh(ky)]^2 + \tanh(ky)\left(\frac{\sigma_{CS}}{\varepsilon_0 v_0}\right)^2}{[1+\tanh(ky)]^2 + \left[\tanh(ky)\frac{\sigma_{CS}}{\varepsilon_0 v_0}\right]^2}. \tag{12}$$

Using these equations we can numerically analyze responds of the SAW sensor.

3. Experiment setup

In experiment we prepared bilayer structures (Fig. 2) for hydrogen detection. On a piezoelectric substrate $LiNbO_3$ (Y–Z cut) ($20\times30\times2$ mm^3) four identical acoustic delay lines are formed (Fig. 3). All interdigital transducers consist of 20 finger pairs, each 20 μm wide and 20 μm gaps between them. The operating frequency of each of the delay lines is about 43.6 MHz and the wavelength is 80 μm. The interdigital transducers are 14 mm apart from each other in each delay line.

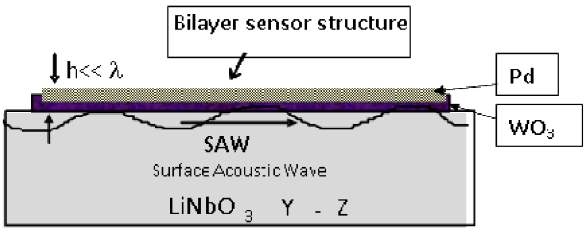

Fig. 2. The bilayer structure of the sensor.

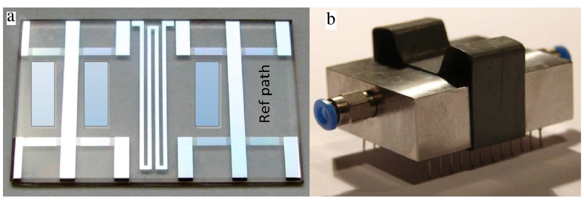

Fig. 3. (a) Four acoustics path on $LiNbO_3$; (b) SAW sensor closed in chamber.

The WO_3 sensors layers with thicknesses of about 50 nm, 100 nm, 150 nm were made on three delay line by means of a vacuum sublimation method, using a special aluminum mask. The vapor source consisted of commercially available WO_3 powder (Fluka 99.9%) and molybdenum heater. The average growing velocity of the film was about 1.5 nm/s and the temperature of the heater was about 1000 °C. A copper–constantan thermocouple was used to control the heater temperature. The thin palladium (Pd) layer (about 10 nm) was made on each WO_3 layer separately by means of vapor deposition in high vacuum after the deposition of the WO_3 film in a new process. During the sublimation the substrate was at room temperature.

In experiment measurements the total gas mixture flow rate of 500 ml/min was used. The volume of the measuring chamber was about 8 cm^3. The sensor was tested in a computer-controlled system. Gases concentrations of 0.5%, 1%, 1.5%, and 2% hydrogen in synthetic air were mixed using mass flow controllers (Bronkhorst Hi-Tech). The temperature of the substrate was measured using a thermocouple adjacent to the sensor structure.

As measured output signals the differential frequencies on the output of the mixer were taken (Fig. 1). Relative changes of the frequency are proportional to the relative changes of the SAW velocity.

4. Experimental results for hydrogen gas

Experimental results are presented below for thicknesses WO_3 sensor layers 50 nm, 100 nm, and 150 nm with 10 nm Pd on each. Output differential frequency signals are showed in Fig. 4. All measurements were carried out at room temperature, about 25 °C, with gas mixture flow rate 100 ml/min through the chamber.

In Fig. 5 there are shown the results in relative scale. We can see that the value of the change in frequency is dependent on concentration of the hydrogen and on the thickness of the sensor layer. We obtained maximum frequency change (output signal from sensor) from 100 nm thick sensor layer but lower values of the output signals were obtained for 50 nm and 150 nm thick layers.

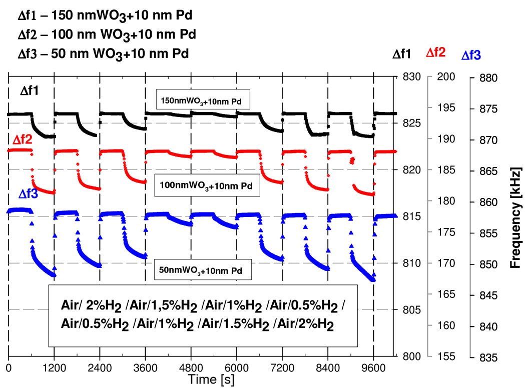

Fig. 4. Experimental results for thickness of the WO_3 + Pd sensor layers 50, 100, 150 nm H_2 gas (2%, 1.5%, 1.0%, 0.5%), $T = 25$ °C.

These results are summarized in Fig. 6.

5. Numerical results

In the numerical analysis of the SAW gas sensor we use Eq. (10) applied in the Python code. The following parameters in the calculations were used: gas concentration, layer thickness and radius of the pores, type of

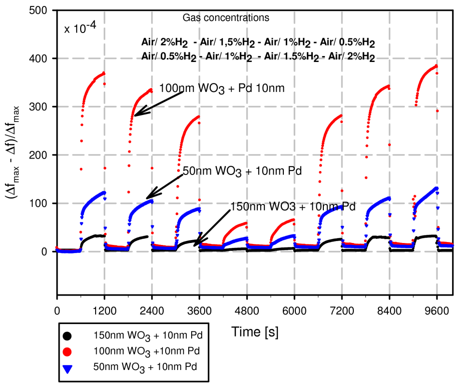

Fig. 5. Experimental results for three layers at thickness 50 nm, 100 nm, 150 nm for various concentration of H_2 gas, $T = 25\,°C$.

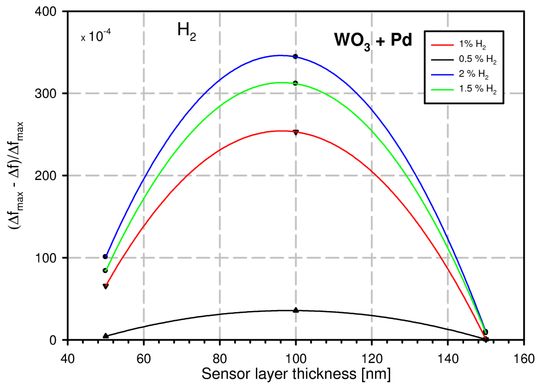

Fig. 6. Experimental results for WO_3 + Pd sensor layers at thickness 50 nm, 100 nm and 150 nm at various concentration of H_2 gas.

the semiconductor layer. We reported the characteristics for hydrogen. As the starting point of the work of the sensor we assumed the conduction of the sensor layer $\sigma_s = v_0 C_S = 4.7 \times 10^{-7}\ \Omega^{-1}$. As a representative radius of pores we use $r = 2$ nm. The numerical results were checked for the thicknesses of the sensor layer 50 nm, 100 nm and 150 nm at the operation temperature 300 K. The sensitivity coefficient value $a = 1\ \text{ppm}^{-1}$ was established.

For graphic presentation of the results we use statement between relative changes of the differential frequency and velocity of the SAW wave as follows:

$$\frac{\Delta f_{\max} - \Delta f}{\Delta f_{\max}} = \kappa \frac{\Delta v_{\max} - \Delta v}{\Delta v_{\max}}\,, \qquad (13)$$

where $\Delta f_{\max}, \Delta v_{\max}$ are the maximum changes of the differential frequency and SAW velocity, respectively, Δf, Δv are changes of the differential frequency and SAW velocity, respectively, κ is scaling parameter.

Numerical results are presented in Fig. 7. We can see that for 0.5% hydrogen concentration optimal layer thickness is in the range 80 nm to 100 nm, and for 1% to 2%

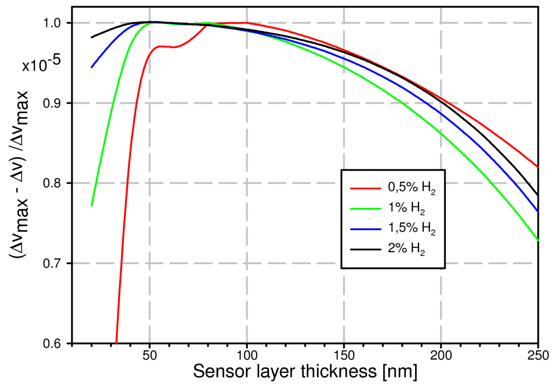

Fig. 7. Relative changes of velocity vs. sensor layer thickness — numerical results. Sensitivity coefficient $a = 1$, temperature 300 K, $\sigma = 4.7 \times 10^{-7}\ \Omega^{-1}$, $k = 10^8\ \text{s}^{-1}$, $D_k = 10^{12}\ \text{nm}^2\ \text{s}^{-1}$, $E_g = 2.7$ eV (for WO_3), $M = 2$ g/mol (H_2).

of the hydrogen concentrations optimal thicknesses are down shifted (50 nm to 80 nm). These numerical results in essential are in good accordance with experimental results depicted in Fig. 6, however it must be taken into account that we have only three points for constructing curves in Fig. 6 (three sensor layers). Accuracy of this picture is not satisfactory, but numerical results are converging with experimental results.

6. Conclusions

a) This paper presents the new sensors bilayer structure WO_3 + Pd for hydrogen detection.

b) Experimental results are compared with numerical analysis SAW gas sensor using theoretical model of the porous sensor layer in SAW configuration.

c) Numerical results are in good accordance with experimental results.

d) Optimal sensor layer thickness depends on gas concentration and is thinner for lower concentrations.

e) Theoretical model presented in [1] may be useful for optimization of the SAW gas sensor structure.

References

[1] T. Hejczyk, M. Urbańczyk, W. Jakubik, *Acta Phys. Pol. A* **118**, 1148 (2010).

[2] M. Penza, G. Cassano, P. Aversa, A. Cusano, M. Consales, M. Giordano, L. Nicolais, *IEEE Sensors J.* **6**, 867 (2006).

[3] M. Penza, P. Aversa, G. Cassano, W. Wlodarski, K. Kalantar-Zadeh, *Sensors Actuators B* **127**, 168 (2007).

[4] W. Jakubik, M. Urbańczyk, S. Kochowski, J. Bodzenta, *Sensors Actuators B* **82**, 265 (2002).

[5] W. Jakubik, M. Urbańczyk, E. Maciak, in: *XX Eurosensors*, Ed. P. Enokssen, University of Goeteborg, Goeteborg 2006, Vol. 1, *Goeteborg*, 2006, p. 124.

[6] D. Amico, A. Palma, E. Verona, in: *IEEE Ultrason. Symp.*, Vol. 1, 1982, p. 308.

[7] A. Venema, E. Nieuwkoop, M.J. Vellekoop, W. Ghijsen, A. Barendsz, M.S. Nieuwenhuizen, *IEEE Trans. Ultrason. Ferroelectr. Freq. Control* **UFFC-34**, 148 (1987).

[8] T. Pustelny, E. Maciak, Z. Opilski, M. Bednorz, *Opt. Appl.* **37**, 187 (2007).

[9] W. Jakubik, *Sensors Actuators B* **96**, 321 (2003).

[10] B.A. Auld, *Acoustic Fields and Waves*, Vol. 2, Wiley, New York 1973.

[11] T. Hejczyk, M. Urbańczyk, W. Jakubik, *Acta Phys. Pol. A* **118**, 1153 (2010).

[12] S. Gordon, A. Kino, *IEEE Trans. Electron Dev.* **ED-18**, 347 (1971).

[13] G. Sakai, N. Matsunaga, E. Shimanoe, N. Yamazone, *Sensors Actuators B* **80**, 125 (2001).

[14] B. Pustelny, T. Pustelny, *Acta Phys. Pol. A* **116**, 383 (2009).

[15] T. Pustelny, A. Opilski, B. Pustelny, *Acta Phys. Pol. A* **114**, A183 (2003).